Published in final edited form as:
Exp Eye Res. 2015 January ; 130: 29–37. doi:10.1016/j.exer.2014.11.007.

Prolonged elevation of intraocular pressure results in retinal ganglion cell loss and abnormal retinal function in mice

A Kareem Khan[a], **Dennis Y Tse**[a], **Meike van der Heijden**[a,b], **Priya Shah**[a], **Derek Nusbaum**[b], **Zhuo Yang**[a], **Samuel M Wu**[a,b], and **Benjamin J Frankfort**[a,*]

[a]Department of Ophthalmology, Baylor College of Medicine, Houston, TX

[b]Department of Neuroscience, Baylor College of Medicine, Houston, TX

Abstract

The purpose of this study was to assess the impact of prolonged intraocular pressure (IOP) elevation on retinal anatomy and function in a mouse model of experimental glaucoma. IOP was elevated by anterior chamber injection of a fixed combination of polystyrene beads and sodium hyaluronate, and maintained via re-injection after 24 weeks. IOP was measured weekly with a rebound tonometer for 48 weeks. Histology was assessed with a combination of retrograde labeling and antibody staining. Retinal physiology and function was assessed with dark-adapted electroretinograms (ERGs). Comparisons between bead-injected animals and various controls were conducted at both 24 and 48 weeks after bead injection. IOP was elevated throughout the study. IOP elevation resulted in a reduction of retinal ganglion cell (RGCs) and an increase in axial length at both 24 and 48 weeks after bead injection. The b-wave amplitude of the ERG was increased to the same degree in bead-injected eyes at both time points, similar to previous studies. The positive scotopic threshold response (pSTR) amplitude, a measure of RGC electrical function, was diminished at both 24 and 48 weeks when normalized to the increased b-wave amplitude. At 48 weeks, the pSTR amplitude was reduced even without normalization, suggesting more profound RGC dysfunction. We conclude that injection of polystyrene beads and sodium hyaluronate causes chronic IOP elevation which results in phenotypes of stable b-wave amplitude increase and progressive pSTR amplitude reduction, as well as RGC loss and axial length elongation.

Keywords

Glaucoma; retinal ganglion cell; scotopic threshold response (STR); electroretinogram (ERG); intraocular pressure (IOP); microbead

*Author for correspondence: benjamin.frankfort@bcm.edu, Baylor College of Medicine, Department of Ophthalmology, 6565 Fannin, NC – 205, Houston, TX, 77030.

Conflict of interest statement:
The authors have no financial interest related to this work.

1. Introduction

Glaucoma is a leading cause of blindness internationally and of increasing public health concern (Quigley and Broman, 2006). The only modifiable risk factor thus far conclusively identified is intraocular pressure (IOP), and the reduction of IOP is known to limit disease onset and slow disease progression (CNTGSG, 1998; Gordon et al., 2002; Leske et al., 2003). Ocular hypertension, defined as a mild, chronic elevation in IOP, can lead to progressive optic nerve and retinal ganglion cell (RGC) changes that impact visual function and optic nerve appearance (Gordon et al., 2002).

To better understand the role of elevated IOP on RGCs and the optic nerve, multiple laboratories have developed murine models of ocular hypertension and glaucoma (Aihara et al., 2003; Chen et al., 2011; Cone et al., 2010; Cone et al., 2012; Frankfort et al., 2013; Gross et al., 2003; Grozdanic et al., 2003; Ji et al., 2005; Ruiz-Ederra and Verkman, 2006; Samsel et al., 2011; Sappington et al., 2010; Urcola et al., 2006). Our preferred model, which makes use of the injection of polystyrene beads followed by sodium hyaluronate into the anterior chamber of a mouse eye as developed by Sappington and modified by Quigley, results in a chronic IOP elevation (Cone et al., 2010; Frankfort et al., 2013; Sappington et al., 2010). This model, and other variations of the “microbead occlusion” model, have similar characteristics including stable IOP increase, limited IOP variation, and neurodegeneration in mice (Chen et al., 2011; Cone et al., 2010; Della Santina et al., 2013; Frankfort et al., 2013; Sappington et al., 2010). The anatomic features of these models include abnormal axonal transport and neurotransmission, axonal loss, RGC loss, and age and species-dependent phenotypes (Chen et al., 2011; Cone et al., 2010; Cone et al., 2012; Crish et al., 2010; Della Santina et al., 2013; Frankfort et al., 2013; Samsel et al., 2011; Sappington et al., 2010). There are few detailed analyses of RGC and inner retinal functional changes in response to chronic IOP elevation in mice, and these studies suggest that RGC-specific functional changes occur, and likely include RGC subtype-specific effects (Della Santina et al., 2013; Feng et al., 2013; Frankfort et al., 2013; Holcombe et al., 2008).

The electroretinogram (ERG) can be used to assess retinal electrical function in living animals. The primary components of the ERG, the a-wave (produced by photoreceptors), and the b-wave (produced by bipolar cells) have been understood for many years. The positive scotopic response (pSTR; produced by RGCs), and the negative scotopic response (nSTR; likely produced by AII amacrine cells) have also been described (Abd-El-Barr et al., 2009; Saszik et al., 2002; Sieving, et al., 1986). The entire system operates under the principle of synaptic convergence; light sensitivity responses increase after every synapse in the direction of electrical transmission (photoreceptors → bipolar cells → RGCs/AII amacrine cells). Thus, the components of the ERG have different levels of sensitivity, with the pSTR and nSTR detectable at the lowest light intensities, and the b-wave and a-wave detectable at relatively brighter light intensities (Abd-El-Barr et al., 2009). Lastly, since the retinal circuitry governing the ERG is well delineated, changes in the ERG can provide evidence not only for dysfunction of the retina as a whole, but for changes to specific pathways or cell types. For example, changes in the pSTR alone might signify an RGC-specific phenotype.

We have previously used a version of the microbead occlusion model to produce chronic IOP elevation in mice. With this model, we identified an IOP-dependent effect on RGC function as measured by the pSTR, a mild b-wave amplitude increase, and anatomic phenotypes of RGC loss and axial length elongation (Frankfort et al., 2013). We extended these studies and assessed long term (24 and 48 week post-injection) effects on RGC structure and function. We report persistent anatomic phenotypes of RGC loss and axial length, and physiologic phenotypes of stable b-wave amplitude increase and progressive pSTR amplitude reduction.

2. Methods

2.1. Animals

6 week old C57Bl/6J female mice were obtained from the Jackson Laboratories and maintained in accordance with the ARVO Statement for the Use of Animals in Ophthalmic and Vision Research, Directive 2010/63/EU, NIH guidelines, and the Baylor College of Medicine IACUC requirements. Mice were maintained in a facility with a temperature of 68–72°F and a light-dark cycle of 12 hours.

2.2. IOP elevation and measurement

All mice were sedated with a weight-based intraperitoneal injection of ketamine (80mg/kg), xylazine (16mg/kg), and acepromazine (1.2mg/kg). The left eye was dilated with a drop of tropicamide 1%. Additional topical anesthesia was achieved with a drop of proparacaine hydrochloride 0.5%. Anterior chamber injection of polystyrene beads was performed as previously described with minor modifications (Cone et al., 2010; Frankfort et al., 2013). A sterile 30 gauge needle was used to puncture the cornea lateral to the dilated pupil margin. A freshly pulled glass micropipette with an inner diameter of 60–75 μm was attached to a Hamilton syringe and advanced through the corneal incision into the anterior chamber. A fixed volume of polystyrene beads (1.5 μl containing 4.7×10^6 of 6 μm beads and 2.4×10^7 of 1 μm beads; Polysciences, Inc., Warrington, PA), followed by 3 μl of sodium hyaluronate (Provisc, Alcon Laboratories, Ft. Worth, TX) was injected into the anterior chamber over a period of 60 seconds. This 1.5 + 3 protocol is similar to the 2 +3 protocol previously reported (Cone et al., 2010; Cone et al., 2012), but was developed independently as we found that it resulted in a lower but more stable IOP elevation compared to other bead volumes. Following bead injection, a drop of moxifloxacin 0.5% was placed on the cornea to prevent infection. To control for the procedure, additional animals received the same injection procedure except the beads were replaced with 1x phosphate-buffered solution (PBS or saline). The right eye was not injected in any animals to serve as an intra-animal control. A subset of animals (those which were not sacrificed at the 24 week time point for experiments and also did not display obvious anterior segment abnormalities such as posterior synechiae or an irregular pupil) received a repeat injection halfway through the expected study. This occurred after 24 weeks and the injection was performed via the same procedure (injection of either polystyrene beads or saline followed by sodium hyaluronate) to the same eye as originally injected. To optimize corneal integrity in these animals, a new corneal incision at least 90 degrees away from the original incision was created with a 30

gauge needle and used as the injection site. Prior to use, beads were washed in 100% ethanol to reduce storage contaminants.

IOP was measured on the day prior to treatment, on the day after treatment and then once each week. IOP was measured for a period of 24 weeks for all animals (n = 49; 35 bead-injected and 14 saline-injected) and for a period of 48 weeks in the group of animals that received repeat injection after 24 weeks (n = 24; 17 bead-injected and 7 saline-injected). IOP was recorded using a rebound tonometer optimized for mouse use (Tonolab, Icare, Finland) as previously described (Frankfort et al., 2013; Pease et al., 2011). To reduce variability, IOP was measured from animals in the same order at the same starting time on the same day of the week. The IOP difference between the eyes was used to quantify the amount of IOP increase after treatment and calculated as previously described (Frankfort et al., 2013).

2.3. Axial Length Measurement/Immunohistochemistry/Cell Counting

Eyes were immediately removed after euthanasia via anesthetic overdose followed by cervical dislocation and the optic nerves trimmed flush with the sclera. Whole eyes were placed cornea down on a slide and the anterior-posterior diameter of the eye (axial length) measured with a camera/controller system (Keyence Corp., Elmwood Park, NJ). The eyes were then rotated 90° along the anterior-posterior axis and re-measured. The average of the two measurements was recorded as the axial length as previously described (Frankfort, et al, 2013).

Prior to immunohistochemistry, some eyes were retrogradely labeled with Neurobiotin as previously described (Frankfort et al., 2013; Pang and Wu, 2011). Eyes were then prepared for immunohistochemistry according to standard techniques. Briefly, retinas were dissected from freshly enucleated eyes in PB++ solution (1x PBS, 0.5% Triton X-100, 0.1% NaN_3), fixed in 4% paraformaldehyde for 1 hour, washed with PB++ for several hours, and blocked in PB++ containing 10% donkey serum at 4° overnight to reduce non-specific binding. At this point, eyes for which sectioned retinas were required were cut into 40–60 μm thick sections with a microtome (Vibratome, Leica Microsystems, Bannockburn, IL). Flat mount or sectioned specimens were treated with PB++ containing 3% donkey serum as well as primary antibody (mouse anti-class III beta-tubulin (TUJ1, 1:500, Covance, Inc.)), if not treated with Neurobiotin, for several days at 4°. Retinas were then washed with PB++ for several hours, and incubated with PB++ containing 3% donkey serum as well as the appropriate combination of secondary antibodies overnight at 4°. Secondary antibodies were Alexa Fluor 488-conjugated donkey anti-mouse (1:300) or Cy3-conjugated strepravidin (1:200, both from Jackson Immunoresearch), and were mixed with the nuclear dye TO-PRO3 (1:4000, Molecular Probes, Eugene, OR) to allow for nuclear staining. Samples were then washed in PB++ for several hours and mounted on a slide and cover slip containing mounting solution (Vectashield, Vector Laboratories).

Images were obtained with a laser confocal microscope (LSM 510) and processed with Zeiss LSM-PC software, ImageJ, and Photoshop (Adobe). For RGC counting, eight regions of each retina were manually counted by an investigator who was masked to the condition of the retina as previously described (Frankfort et al., 2013). Each retinal region had an area of 0.053 mm^2, which enabled conversion to cells/mm^2.

2.4. Electroretinogram (ERG) Recordings

After dark-adapting for at least 2 hours, under dim red light, mice were prepared for ERG testing as described previously (Abd-El-Barr et al., 2009; Frankfort et al., 2013; Pennesi et al., 2003). Signals were amplified, data acquired, and traces analyzed with a Grass P122 amplifier, bandpass 0.1 to 1,000 Hz (Grass Instruments, West Warwick, RI), a National Instruments data acquisition board (sampling rate = 10,000 Hz), and custom software written in Matlab (MathWorks, Natick, MA), respectively. Scotopic range flashes were produced with cyan emitting diodes that had been calibrated with a photometer. Flashes were converted to the unit photoisomerizations/rod (1 scot cd m^2 = 581 photoisomerizations/rod/s)(Abd-El-Barr et al., 2009; Lyubarsky et al., 2004; Saszik et al., 2002). 500 nm wavelength light for a duration of 0.5 milliseconds was used for all flashes. To remove oscillatory potentials, the scotopic b-wave was digitally filtered (low-pass filter; Fc = 60 Hz). The positive scotopic threshold response (pSTR) and negative scotopic threshold response (nSTR) were measured at similar range of signal strengths as previously described (Abd-El-Barr et al., 2009; Frankfort et al., 2013). A log intensity scale where log 10^0 = 1 photoisomerization/rod is used throughout the manuscript to describe stimulus strength.

The b-wave amplitude ratio and the similar a-wave amplitude ratio were determined as previously described for each animal using the following equation (Frankfort et al., 2013):

$$b-wave\ amplitude\ ratio = mean\ b-wave_{injected} / mean\ b-wave_{uninjected} \quad \text{(Equation 1)}$$

The mean b-wave was calculated as the average of the b-wave amplitudes obtained at six different sub-saturation stimuli ranging on the log intensity scale from 0.203 to 2.87 (1.6 to 7.5×10^2 photoisomerizations/rod). The same stimuli were used to obtain the amplitudes of the a-wave. pSTR and nSTR measurements were obtained at three stimuli ranging from log intensity − 1.91 to −1.04 (1.2×10^{-2} to 9.1×10^{-2} photoisomerizations/rod)(Abd-El-Barr et al., 2009). pSTR and nSTR measurements from the uninjected eye were subtracted from the injected eye of the same animal in order to calculate the pSTR or nSTR amplitude difference. To account for an increased b-wave amplitude, normalization of the STR according to the b-wave amplitude ratio was then performed in order to calculate the normalized pSTR or nSTR amplitude difference as previously described (Frankfort et al., 2013). With or without normalization, a more negative pSTR or nSTR amplitude difference represents a greater reduction from the contralateral, uninjected eye.

2.5. Statistical Analysis

Analyses were performed with SPSS Version 21 (IBM). Statistical tests were either an ANOVA with repeated measures or a t-test of independent samples as indicated. A cutoff of $p < 0.05$ was used as significant for all analyses.

3. Results

3.1. IOP comparison of bead-injected, saline-injected, and uninjected mice

We sought to determine if additional exposure to elevated IOP beyond 12 weeks caused additional RGC loss and inner retinal dysfunction. To accomplish this, 35 animals received a single injection of a combination of polystyrene beads and sodium hyaluronate, and 14 animals received a single injection of saline and sodium hyaluronate to serve as controls (Methods). Bead injection resulted in a statistically significant increase in IOP when compared to contraleteral, uninjected control eyes (ANOVA with repeated measures, $p < 0.001$, Figure 1A, Table 1). The mean IOP of bead-injected, saline-injected and uninjected eyes across all time points were 13.4, 11.2, and 10.6 mmHg, respectively, and the mean IOP difference between bead-injected and uninjected eyes across all time points was 2.7 mmHg (25.4% increase; Table 1). This magnitude of elevation was consistent with reported elevations using a similar procedure (Methods)(Cone et al., 2012). The magnitude of IOP elevation after bead injection varied during the study and was lowest in the second 12 week period (weeks 13–24; Figure 1A; Table 1). Others have used re-injection of beads in analogous systems to maintain elevated levels of IOP (Sappington et al., 2010). Therefore, to prevent further IOP reduction we re-injected all animals that were to be followed in our 48 week study with additional beads and sodium hyaluronate following the 24 week time point (Methods). After re-injection, IOP returned to levels similar to those seen during the first 12 weeks of the study and remained stable for the final 24 weeks (Table 1). When the average IOP elevation across 12 week periods were compared to one another, no differences in IOP elevation were detected except between the second (weeks 13–24) and fourth (weeks 37–48) periods, which were the lowest and highest periods of IOP elevation, respectively (Table 1). There were only eight total IOP spikes (mmHg > 30) in the entire study.

To estimate the amount of additional IOP exposure that occurred in injected eyes, we calculated the cumulative IOP difference for each animal (Equation 1). Bead-injected animals were exposed to a greater cumulative IOP difference than saline-injected animals at both 24 weeks and 48 weeks after injection (t test, $p < 0.001$; Figure 1B; Table 1). Since the magnitude of IOP elevation was slightly higher after re-injection, animals were exposed to a higher cumulative IOP difference in the second half of the study.

3.2. Retinal ganglion cell counts

In order to determine if prolonged exposure to IOP elevation resulted in RGC loss, we performed retrograde labeling of RGC axons with Neurobiotin in freshly enucleated eyes using an established protocol (Methods)(Frankfort et al., 2013; Pang and Wu, 2011). After 24 weeks of IOP elevation, we noted a 14.4% reduction in RGCs compared to contralateral uninjected controls which was equivalent between the mid-retina and periphery (Figure 2A and 2B; Table 2; $p < 0.01$ for RGCs compared to uninjected controls; $p = 0.887$ for mid-retina vs. periphery). We attempted to perform Neurobiotin labeling in animals exposed to 48 weeks of IOP elevation but were unsuccessful as Neurobiotin uptake in treated eyes was extremely poor in these older animals (our unpublished observations). We therefore counterstained retinas exposed to 48 weeks of elevated IOP with an antibody to class III beta-tubulin (TUJ1) in order to exogenously label RGCs. We detected a 19.4% reduction in

RGCs compared to contralateral uninjected controls, which was again equivalent between the mid-retina and periphery (Figure 2C and 2D; Table 2; $p < 0.001$ for RGCs compared to uninjected controls; $p = 0.679$ for mid-retina vs. periphery). We did not detect a correlation between cumulative IOP exposure and RGC loss (Pearson's correlation with $p = 0.356$ at 24 weeks and $p = 0.338$ at 48 weeks). Retinas stained with TUJ1 tend to label more RGCs then Neurobiotin, even in young animals, which explains the higher number of RGCs in both treated and control eyes (Table 2). To assess the gross effects of elevated IOP on other retinal layers, we performed nuclear staining with TO-PRO3 in retinal cross sections at the latest (48 week) time point (Figures 2E and 2F). The thickness and appearance of both the inner and outer nuclear layers was unchanged following IOP elevation.

3.3. Axial lengths

We and others have reported a progressive increase in axial length in animals exposed to elevated IOP over time (Chou et al., 2011; Cone et al., 2010; Frankfort et al., 2013). At 24 weeks, we found an axial length increase in bead-injected eyes of 0.14 mm when compared to contralateral, uninjected controls (Table 2); this is similar to the increase in axial length we found at 6 and 12 weeks (Frankfort et al., 2013). We previously hypothesized that the majority of the axial length increase seen in this model occurred within the first 6 weeks and then stabilized, and our finding at 24 weeks are consistent with this hypothesis. We observed an axial length increase in bead-injected eyes of 0.19 mm when compared to controls at the later 48 week time point (Table 2). An ANOVA comparing axial length increases after 24 and 48 weeks did not show an interaction effect between treatment and duration of exposure. This suggests that axial length elongation remains approximately stable after the initial bead injection, despite the additional injection at 24 weeks and the higher IOP exposure in the second 24 week period.

3.4. ERG comparisons

Multiple groups have reported ERG abnormalities in rodents with experimental glaucoma (Bui et al., 2005; Fortune et al., 2004; Frankfort et al., 2013; Holcombe et al., 2008; Porciatti et al., 2010; Porciatti et al., 2007; Saleh et al., 2007). We recently found that the scotopic b-wave amplitude, but not the a-wave amplitude, is increased shortly after IOP elevation, and that the pSTR amplitude is diminished in a cumulative IOP dependent manner (Frankfort et al., 2013). Accordingly, we sought to determine if these physiological changes progressed with prolonged exposure to IOP elevation. At both 24 and 48 weeks after injection, the b-wave amplitude was increased in bead-injected eyes compared to both uninjected and saline injected eyes (Figure 3A; ANOVA with repeated measures comparing all three groups, $p = 0.031$ and 0.021, at 24 and 48 weeks, respectively; $p = 0.019$ and 0.003 for bead injected vs. uninjected eyes only; and $p = 0.049$ and 0.024 for bead vs. saline injected eyes only). Furthermore, the magnitude of the b-wave increased with increasing light intensity, but the magnitude of this growth was not altered by treatment (ANOVA; $p = 0.701$ and $p=0.409$ for within subjects effects of treatment on b-wave amplitude for 24 weeks and 48 weeks, respectively). Similar to our previous study, inter-animal comparisons showed no difference in the amplitudes of the a-wave, pSTR, or nSTR (Figure 3A, $p > 0.05$ for all time points and comparisons). We used the b-wave amplitude ratio (Figure 3B; Methods) to determine the average intra-animal b-wave increase after bead injection. The increase in b-wave amplitude

was constant at the two time points (ANOVA with repeated measures with $p > 0.05$), and also unchanged from published data in younger animals with shorter duration of IOP exposure (Frankfort et al., 2013). These data suggest that the early effects on the b-wave do not alter with time.

Since ERG light sensitivity responses increase with each layer of the retina, an increased b-wave amplitude should be accompanied by concomitant increases in the amplitudes of the pSTR and nSTR. We did not see such increases (Figure 3A), and hypothesized that this might be due to inter-animal variation. To control for inter-animal variation, we therefore compared the pSTR and nSTR amplitudes between injected (bead or saline) and contralateral uninjected eyes and calculated the pSTR and nSTR amplitude difference for each animal (Methods; Frankfort et al., 2013). We then compared the pSTR and nSTR amplitude differences between bead-injected and saline-injected animals at both 24 and 48 weeks (Figure 4A). We detected no change in the pSTR amplitude difference at 24 weeks and no change the nSTR amplitude difference at either 24 or 48 weeks. However, at 48 weeks, there was a statistically significant reduction in the pSTR amplitude difference across all light intensities which occurred in an intensity dependent fashion; the amount of reduction increased with brighter light stimulus. Since this reduction occurred in the presence of an increased b-wave amplitude, it is suggestive of very strongly decreased RGC function. To get a better sense of this decrease in RGC function and to further account for the increased b-wave amplitude, we normalized the pSTR and nSTR to the b-wave and recalculated the pSTR and nSTR amplitude difference for each animal (Methods; Frankfort, et al., 2013). When normalized to the b-wave, we now detected a reduction in the pSTR amplitude difference across all light intensities at both time points (Figure 4B). This confirmed that RGC function was decreased at 48 weeks and suggested that RGC function was also decreased by the earlier 24 week time point. The nSTR amplitude difference was reduced with this normalization as well, but the results were not statistically significant. Taken together, these data suggest that RGC function decreases progressively from 24 to 48 weeks.

4. Discussion

Our version of the microbead occlusion model yields a consistent elevation of IOP with a single injection which diminishes slightly after about 12 weeks, and can be extended out to 48 weeks with a second injection of beads after 24 weeks (Cone et al., 2012). This injection protocol is different from our previous study, which used a wider range of fluid volume during injection, and resulted in slightly lower IOP elevations than previously obtained (Frankfort, et al., 2013). By using a protocol designed to avoid large IOP increases and IOP spikes which can cause severe ocular phenotypes, this approach provides a mechanism to study the long-term effects of elevated IOP, as well as the incremental effects of elevated IOP at multiple time points.

We and others have detected mild amounts of RGC loss in young C57Bl/6J mice when using a combination of polystyrene beads and sodium hyaluronate (Cone et al., 2010; Cone et al., 2012; Frankfort et al., 2013). This study is the first to carry analogous experiments of injections in young animals out to extreme time points of 24 and 48 weeks after injection.

We assessed RGC loss at both 24 and 48 weeks after bead injection and detected a 14.4% and 19.4% loss of RGCs, respectively. Thus, there was only a minimal increase in RGCs losses following an additional 24 weeks of IOP exposure, despite the fact that IOPs were higher in the second 24 week period (Figure 1, Table 1). One explanation for this observation is that C57Bl/6J mice appear to have a strain-dependent resistance to the effects of IOP elevation and also appear to be less susceptible to IOP effects when of older age (Cone et al., 2010; Cone et al., 2012). It is therefore possible that these genetic factors minimize additional RGC loss despite the prolonged period of exposure. Our inability to detect Neurobiotin retrograde labeling in older mice (48 weeks) also supports previous observations that axonal injury can occur even as RGC somas are preserved in RGCs exposed to elevated IOP (Buckingham et al., 2008; Soto et al., 2008). Accordingly, it is also possible that the older retinas in this study have very abnormal axon function despite the only mild reduction in RGC somas. Finally, because of limitations in Neurobiotin-based RGC soma staining at 48 weeks, it is possible that the additional increase in RGC loss at 48 weeks is a consequence of the change in assay used and not prolonged IOP exposure.

Our earlier study on ERG changes in response to IOP elevation identified both a b-wave amplitude increase which we attributed to an early loss of an amacrine cell derived negative component of the ERG and a pSTR amplitude decrease that occurred in a cumulative IOP-dependent manner which we attributed to RGC dysfunction that preceded RGC loss (Frankfort et al., 2013). The current study found differing effects of long-term IOP exposure on these two ERG components.

In this study, the b-wave amplitude was increased to the same level as was observed with short term IOP exposure. The magnitude of the b-wave increase was unchanged with duration of exposure to IOP elevation and there was no gross change in bipolar cell appearance in the inner nuclear layer. We also saw mild (not statistically significant) effects on the nSTR that were not progressive in this study which support some perturbation of amacrine cell function in which the core electrical activity of AII amacrine cells as measured by the full field flash ERG was maintained. These observations support our previous hypothesis that the b-wave amplitude increase is caused by the loss of an amacrine cell derived negative component of the ERG (Abd-El-Barr et al., 2009; Frankfort et al., 2013). Since the inhibition of Muller cell potassium channels has also been associated with the loss of electronegative ERG components in both cats and rats, another possibility is that Muller cell function or potassium buffering is altered by elevated IOP (Frishman and Steinberg, 1989; Green and Kapousta-Bruneau, 1999). Finally, it is possible that the increased b-wave amplitude results from a subtle increase in upstream photoreceptor sensitivity which is not apparent in the a-wave amplitude. Regardless, the underlying process seems to show a hypersensitive but plateau response to IOP change, since the b-wave changes occur early, show prolonged abnormality, and are not progressive. Single cell recordings under specific experimental conditions will be helpful to distinguish from among these possibilities.

We also found that the pSTR amplitude difference was reduced at 48 weeks and the normalized pSTR amplitude difference was reduced at both 24 and 48 weeks of IOP exposure (Figure 4). Our ability to detect a reduced pSTR in the presence of an increased b-wave at 48 weeks is particularly striking, and suggests that RGC dysfunction may be

considerable. Taken together, these data suggest that RGC dysfunction is progressive with duration of IOP exposure, and support the use of a normalized pSTR to detect early changes in RGC function. Interestingly, these ERG findings occur in the setting of only minimally progressive RGC loss in a genetically and age-resistant mouse strain. Thus, RGC dysfunction after 48 weeks of IOP exposure may also be disproportionate to anatomic changes. Other investigators studying ERG changes in response to IOP elevation using different animal models have found that the innermost retinal components (such as RGCs) are more sensitive to IOP elevation than are the outer cell types (such as photoreceptors (Bui, et al., 2005, Bui, et al., 2013; He, et al., 2006; He, et al., 2008; Holcombe, et al., 2008, Kong, et al., 2009). Furthermore, at least two groups have reported a differential susceptibility to IOP-related functional change among RGC subtypes, suggesting that certain RGCs are more sensitive to IOP elevation than others (Della Santina et al., 2013; Feng et al., 2013). In all of these studies, the IOP achieved was higher than in the present study. Despite these higher IOPs, the observed physiologic changes were not always associated with corresponding anatomic abnormalities, further supporting our observation that changes in RGC function can be detected in a manner which is at times distinct from or disproportionate to anatomic changes. It will be important to assess the effects of prolonged IOP elevation on RGC subtypes with extra- and intra-cellular recording techniques and the integrate those effects with those seen in animals exposed to moderate, short-term IOP elevation in order to best determine the relative changes that occur among RGC subtypes under glaucomatous conditions.

Potential weaknesses of this study are that the magnitude of IOP elevation was not consistent throughout the entire study, and that a re-injection of beads was required to maintain IOP elevation in the second 24 weeks of the study. Others have used re-injection as a mechanism to prolong IOP elevation, and have reported that the IOP levels remained consistent with the second injection (Sappington et al., 2010). We found slightly higher IOP levels after re-injection. This discrepancy may due to the techniques of bead injection used or the time beyond initial injection at which re-injection occurred. Experiments that prevent additional injections yet also maintain a constant level of IOP elevation may be required to make these determinations.

The patterns of electrical dysfunction we observe in this study may correlate with several of the core visual changes that occur in human glaucoma. Vision under dim lighting (scotopic) conditions requires a functioning rod photoreceptor pathway, which integrates electrical signals to the RGCs via the AII amacrine cells (Crooks and Kolb, 1992; Pang et al., 2003; Pourcho and Owczarzak, 1991; Veruki and Hartveit, 2002). If AII amacrine cell activity is disrupted with IOP elevation, one would predict that visual abnormalities in the dark were a component of glaucoma. Indeed this is the case, as several reports implicate dark vision problems in patients with glaucoma, even in the early stages (Lee et al., 1998; Nelson et al., 1999; Ramulu et al., 2009). We also found that scotopic RGC function was increasingly abnormal, which could worsen these problems with dark vision over time.

In this version of the microbead occlusion model, IOP is elevated and remains so for at least 48 weeks following a second bead injection after 24 weeks. The model is defined by slowly increasing RGC damage which is associated with progressive inner retinal electrical

dysfunction as measured by the pSTR. As the phenotypes in this study develop over a much longer period of time than previous reports, our model may therefore provide an opportunity to study the mechanism of disease modulation at multiple time points over a period of many months. Since most patients with glaucoma are treated after unknowingly having the disease for many years and after significant RGC loss is believed to have occurred, opportunities to study the effects of IOP elevation at multiple time points is potentially valuable (Quigley and Green, 1979; Sommer et al., 1991; Varma et al., 2004). This model, in which RGCs are slowly lost in the presence of measurable and increasing electrical dysfunction, may offer such an opportunity.

Acknowledgments

Support for this work was provided by National Institutes of Health Grants EY019908, EY04446, and EY02520 (to S.M.W.) and EY021479 (to B.J.F.); Retina Research Foundation Pilot Study Grants (Houston, TX, to B.J.F. and S.M.W.); Research to Prevent Blindness, Inc. (New York, NY, to B.J.F. and S.M.W.); and an International Retinal Research Foundation Loris and David Rich Award (Birmingham, AL, to D.Y.T.).

References

Abd-El-Barr MM, Pennesi ME, Saszik SM, Barrow AJ, Lem J, Bramblett DE, Paul DL, Frishman LJ, Wu SM. Genetic dissection of rod and cone pathways in the dark-adapted mouse retina. J Neurophysiol. 2009; 102:1945–1955. [PubMed: 19587322]

Aihara M, Lindsey JD, Weinreb RN. Experimental mouse ocular hypertension: establishment of the model. Invest Ophthalmol Vis Sci. 2003; 44:4314–4320. [PubMed: 14507875]

Buckingham BP, Inman DM, Lambert W, Oglesby E, Calkins DJ, Steele MR, Vetter ML, Marsh-Armstrong N, Horner PJ. Progressive ganglion cell degeneration precedes neuronal loss in a mouse model of glaucoma. J Neurosci. 2008; 28:2735–2744. [PubMed: 18337403]

Bui BV, Edmunds B, Cioffi GA, Fortune B. The gradient of retinal functional changes during acute intraocular pressure elevation. Invest Ophthalmol Vis Sci. 2005; 46:202–213. [PubMed: 15623775]

Bui BV, Batcha AH, Fletcher E, Wong VH, Fortune B. Relationship between the magnitude of intraocular pressure during an episode of acute elevation and retinal damage four weeks later in rats. Plos One. 2013; 8:e70513. [PubMed: 23922999]

Chen H, Wei X, Cho KS, Chen G, Sappington R, Calkins DJ, Chen DF. Optic neuropathy due to microbead-induced elevated intraocular pressure in the mouse. Invest Ophthalmol Vis Sci. 2011; 52:36–44. [PubMed: 20702815]

Chou TH, Kocaoglu OP, Borja D, Ruggeri M, Uhlhorn SR, Manns F, Porciatti V. Postnatal elongation of eye size in DBA/2J mice compared with C57BL/6J mice: in vivo analysis with whole-eye OCT. Invest Ophthalmol Vis Sci. 2011; 52:3604–3612. [PubMed: 21372015]

CNTGSG. The effectiveness of intraocular pressure reduction in the treatment of normal-tension glaucoma. Collaborative Normal-Tension Glaucoma Study Group. Am J Ophthalmol. 1998; 126:498–505. [PubMed: 9780094]

Cone FE, Gelman SE, Son JL, Pease ME, Quigley HA. Differential susceptibility to experimental glaucoma among 3 mouse strains using bead and viscoelastic injection. Exp Eye Res. 2010; 91:415–424. [PubMed: 20599961]

Cone FE, Steinhart MR, Oglesby EN, Kalesnykas G, Pease ME, Quigley HA. The effects of anesthesia, mouse strain and age on intraocular pressure and an improved murine model of experimental glaucoma. Exp Eye Res. 2012; 99C:27–35. [PubMed: 22554836]

Crish SD, Sappington RM, Inman DM, Horner PJ, Calkins DJ. Distal axonopathy with structural persistence in glaucomatous neurodegeneration. Proc Natl Acad Sci U S A. 2010; 107:5196–5201. [PubMed: 20194762]

Crooks J, Kolb H. Localization of GABA, glycine, glutamate and tyrosine hydroxylase in the human retina. J Comp Neurol. 1992; 315:287–302. [PubMed: 1346792]

Della Santina L, Inman DM, Lupien CB, Horner PJ, Wong RO. Differential progression of structural and functional alterations in distinct retinal ganglion cell types in a mouse model of glaucoma. J Neurosci. 2013; 33:17444–17457. [PubMed: 24174678]

Feng L, Zhao Y, Yoshida M, Chen H, Yang JF, Kim TS, Cang J, Troy JB, Liu X. Sustained ocular hypertension induces dendritic degeneration of mouse retinal ganglion cells that depends on cell type and location. Invest Ophthalmol Vis Sci. 2013; 54:1106–1117. [PubMed: 23322576]

Fortune B, Bui BV, Morrison JC, Johnson EC, Dong J, Cepurna WO, Jia L, Barber S, Cioffi GA. Selective ganglion cell functional loss in rats with experimental glaucoma. Invest Ophthalmol Vis Sci. 2004; 45:1854–1862. [PubMed: 15161850]

Frankfort BJ, Khan AK, Tse DY, Chung I, Pang JJ, Yang Z, Gross RL, Wu SM. Elevated intraocular pressure causes inner retinal dysfunction before cell loss in a mouse model of experimental glaucoma. Invest Ophthalmol Vis Sci. 2013; 54:762–770. [PubMed: 23221072]

Frishman LJ, Steinberg RH. Intraretinal analysis of the threshold dark-adapted ERG of cat retina. J Neurophysiol. 1989; 61:1221–1232. [PubMed: 2746322]

Gordon MO, Beiser JA, Brandt JD, Heuer DK, Higginbotham EJ, Johnson CA, Keltner JL, Miller JP, Parrish RK 2nd, Wilson MR, Kass MA. The Ocular Hypertension Treatment Study: baseline factors that predict the onset of primary open-angle glaucoma. Arch Ophthalmol. 2002; 120:714–720. discussion 829–730. [PubMed: 12049575]

Green DG, Kapousta-Bruneau NV. A dissection of the electroretinogram from the isolated rat retina with microelectrodes and drugs. Vis Neurosci. 1999; 16:727–741. [PubMed: 10431921]

Gross RL, Ji J, Chang P, Pennesi ME, Yang Z, Zhang J, Wu SM. A mouse model of elevated intraocular pressure: retina and optic nerve findings. Trans Am Ophthalmol Soc. 2003; 101:163–169. discussion 169–171. [PubMed: 14971574]

Grozdanic SD, Betts DM, Sakaguchi DS, Allbaugh RA, Kwon YH, Kardon RH. Laser-induced mouse model of chronic ocular hypertension. Invest Ophthalmol Vis Sci. 2003; 44:4337–4346. [PubMed: 14507878]

He Z, Bui BV, Vingrys AJ. The rate of functional recovery from acute IOP elevation. Invest Ophthalmol Vis Sci. 2006; 47:4872–4880. [PubMed: 17065501]

He Z, Bui BV, Vingrys AJ. Effect of repeated IOP challenge on rat retinal function. Invest Ophthalmol Vis Sci. 2008; 49:3026–3034. [PubMed: 18326699]

Holcombe DJ, Lengefeld N, Gole GA, Barnett NL. Selective inner retinal dysfunction precedes ganglion cell loss in a mouse glaucoma model. Br J Ophthalmol. 2008; 92:683–688. [PubMed: 18296504]

Ji J, Chang P, Pennesi ME, Yang Z, Zhang J, Li D, Wu SM, Gross RL. Effects of elevated intraocular pressure on mouse retinal ganglion cells. Vision Res. 2005; 45:169–179. [PubMed: 15581918]

Kong YX, Crowston JG, Vingrys AJ, Trounce IA, Bui VB. Functional changes in the retina during and after acute intraocular pressure elevation in mice. Invest Ophthalmol Vis Sci. 2009; 50:5732–5740. [PubMed: 19643960]

Lee BL, Gutierrez P, Gordon M, Wilson MR, Cioffi GA, Ritch R, Sherwood M, Mangione CM. The Glaucoma Symptom Scale. A brief index of glaucoma-specific symptoms. Arch Ophthalmol. 1998; 116:861–866. [PubMed: 9682698]

Leske MC, Heijl A, Hussein M, Bengtsson B, Hyman L, Komaroff E. Factors for glaucoma progression and the effect of treatment: the early manifest glaucoma trial. Arch Ophthalmol. 2003; 121:48–56. [PubMed: 12523884]

Lyubarsky AL, Daniele LL, Pugh EN Jr. From candelas to photoisomerizations in the mouse eye by rhodopsin bleaching in situ and the light-rearing dependence of the major components of the mouse ERG. Vision Res. 2004; 44:3235–3251. [PubMed: 15535992]

Nelson P, Aspinall P, O'Brien C. Patients' perception of visual impairment in glaucoma: a pilot study. Br J Ophthalmol. 1999; 83:546–552. [PubMed: 10216052]

Pang JJ, Gao F, Wu SM. Light-evoked excitatory and inhibitory synaptic inputs to ON and OFF alpha ganglion cells in the mouse retina. J Neurosci. 2003; 23:6063–6073. [PubMed: 12853425]

Pang JJ, Wu SM. Morphology and immunoreactivity of retrogradely double-labeled ganglion cells in the mouse retina. Invest Ophthalmol Vis Sci. 2011; 52:4886–4896. [PubMed: 21482641]

Pease ME, Cone FE, Gelman S, Son JL, Quigley HA. Calibration of the TonoLab tonometer in mice with spontaneous or experimental glaucoma. Invest Ophthalmol Vis Sci. 2011; 52:858–864. [PubMed: 20720229]

Pennesi ME, Cho JH, Yang Z, Wu SH, Zhang J, Wu SM, Tsai MJ. BETA2/NeuroD1 null mice: a new model for transcription factor-dependent photoreceptor degeneration. J Neurosci. 2003; 23:453–461. [PubMed: 12533605]

Porciatti V, Chou TH, Feuer WJ. C57BL/6J, DBA/2J, and DBA/2J.Gpnmb mice have different visual signal processing in the inner retina. Mol Vis. 2010; 16:2939–2947. [PubMed: 21203347]

Porciatti V, Saleh M, Nagaraju M. The pattern electroretinogram as a tool to monitor progressive retinal ganglion cell dysfunction in the DBA/2J mouse model of glaucoma. Invest Ophthalmol Vis Sci. 2007; 48:745–751. [PubMed: 17251473]

Pourcho RG, Owczarzak MT. Connectivity of glycine immunoreactive amacrine cells in the cat retina. J Comp Neurol. 1991; 307:549–561. [PubMed: 1869631]

Quigley HA, Broman AT. The number of people with glaucoma worldwide in 2010 and 2020. Br J Ophthalmol. 2006; 90:262–267. [PubMed: 16488940]

Quigley HA, Green WR. The histology of human glaucoma cupping and optic nerve damage: clinicopathologic correlation in 21 eyes. Ophthalmology. 1979; 86:1803–1830. [PubMed: 553256]

Ramulu PY, West SK, Munoz B, Jampel HD, Friedman DS. Driving cessation and driving limitation in glaucoma: the Salisbury Eye Evaluation Project. Ophthalmology. 2009; 116:1846–1853. [PubMed: 19592110]

Ruiz-Ederra J, Verkman AS. Mouse model of sustained elevation in intraocular pressure produced by episcleral vein occlusion. Exp Eye Res. 2006; 82:879–884. [PubMed: 16310189]

Saleh M, Nagaraju M, Porciatti V. Longitudinal evaluation of retinal ganglion cell function and IOP in the DBA/2J mouse model of glaucoma. Invest Ophthalmol Vis Sci. 2007; 48:4564–4572. [PubMed: 17898279]

Samsel PA, Kisiswa L, Erichsen JT, Cross SD, Morgan JE. A novel method for the induction of experimental glaucoma using magnetic microspheres. Invest Ophthalmol Vis Sci. 2011; 52:1671–1675. [PubMed: 20926815]

Sappington RM, Carlson BJ, Crish SD, Calkins DJ. The microbead occlusion model: a paradigm for induced ocular hypertension in rats and mice. Invest Ophthalmol Vis Sci. 2010; 51:207–216. [PubMed: 19850836]

Saszik SM, Robson JG, Frishman LJ. The scotopic threshold response of the dark-adapted electroretinogram of the mouse. J Physiol. 2002; 543:899–916. [PubMed: 12231647]

Sieving PA, Frishman LJ, Steinberg RH. Scotopic threshold response of the proximal retina in cat. J Neurophysiol. 1986; 56:1049–1061. [PubMed: 3783228]

Sommer A, Tielsch JM, Katz J, Quigley HA, Gottsch JD, Javitt J, Singh K. Relationship between intraocular pressure and primary open angle glaucoma among white and black Americans. The Baltimore Eye Survey. Arch Ophthalmol. 1991; 109:1090–1095. [PubMed: 1867550]

Soto I, Oglesby E, Buckingham BP, Son JL, Roberson ED, Steele MR, Inman DM, Vetter ML, Horner PJ, Marsh-Armstrong N. Retinal ganglion cells downregulate gene expression and lose their axons within the optic nerve head in a mouse glaucoma model. J Neurosci. 2008; 28:548–561. [PubMed: 18184797]

Urcola JH, Hernandez M, Vecino E. Three experimental glaucoma models in rats: comparison of the effects of intraocular pressure elevation on retinal ganglion cell size and death. Exp Eye Res. 2006; 83:429–437. [PubMed: 16682027]

Varma R, Ying-Lai M, Francis BA, Nguyen BB, Deneen J, Wilson MR, Azen SP. Prevalence of open-angle glaucoma and ocular hypertension in Latinos: the Los Angeles Latino Eye Study. Ophthalmology. 2004; 111:1439–1448. [PubMed: 15288969]

Veruki ML, Hartveit E. AII (Rod) amacrine cells form a network of electrically coupled interneurons in the mammalian retina. Neuron. 2002; 33:935–946. [PubMed: 11906699]

Highlights

We studied mice exposed to mildly elevated IOP for 24 or 48 weeks.

We examined changes in RGC number, axial length, and the ERG.

RGC loss and axial length increase are mild at both time points.

B wave amplitude increases are similar at both time points.

Positive STR reductions are mild after 24 weeks but severe after 48 weeks.

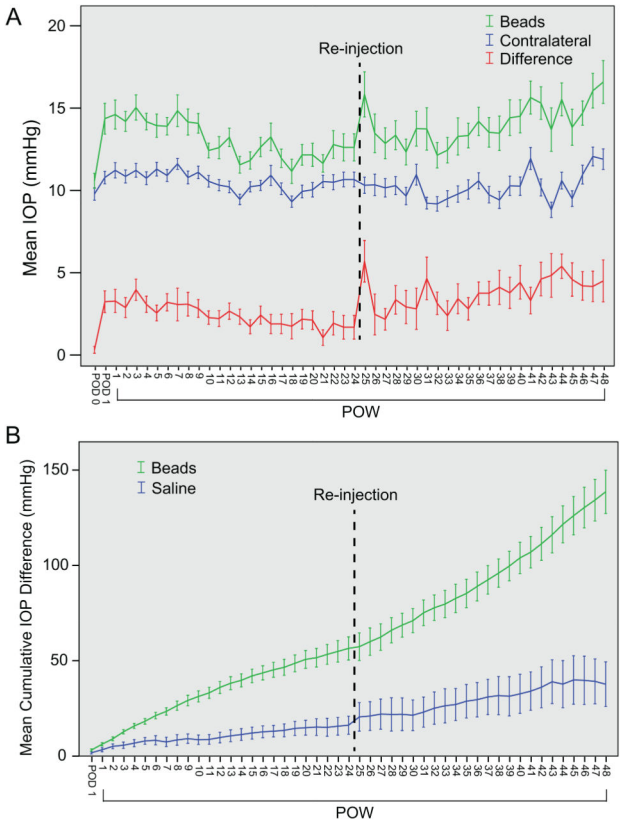

Figure 1. Bead Injection results in prolonged IOP elevation

A. Mean IOP ± SEM. Animals that were to be maintained for 48 weeks were re-injected (dotted line) after 24 weeks. Mean IOP for bead-injected eyes ("Beads," green), contralateral uninjected eyes ("Contralateral," blue), and their difference ("Difference," red) is presented. Bead injection results in a statistically significant IOP elevation (ANOVA with repeated measures, $p < 0.001$). B. Mean Cumulative IOP difference ± SEM. Bead-injected eyes (green) are subject to a statistically larger cumulative IOP than are saline-injected eyes (blue; ANOVA with repeated measures, $p < 0.001$).

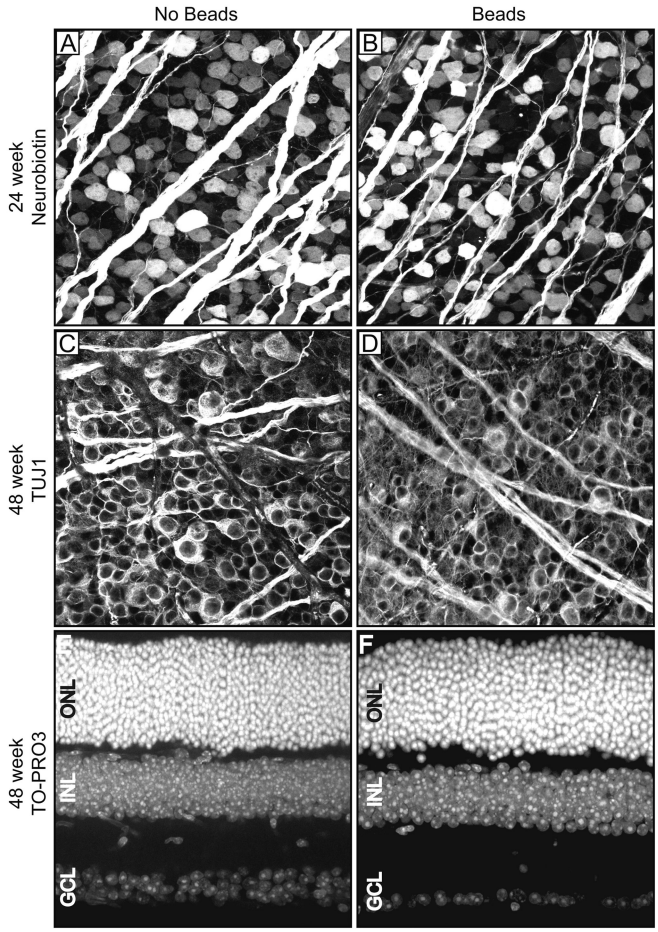

Figure 2. Prolonged IOP elevation results in RGC loss

Examples of uninjected eyes ("No Beads"; panels A, C, E) and bead-injected eyes ("Beads"; panels B, D, F) are presented side by side at 24 weeks after injection (panels A and B), or 48 weeks after injection (panels C–F). A–D. Retinal flat mounts. E, F. Retinal cross sections. A, B. Neurobiotin-staining. C, D. TUJ1-staining. E, F. TO-PRO3 staining. An extreme example of RGC loss (F) is shown in comparison with a typical control retina (E). The INL and ONL are of equivalent thickness. ONL = outer nuclear layer; INL = inner nuclear layer; GCL = ganglion cell layer.

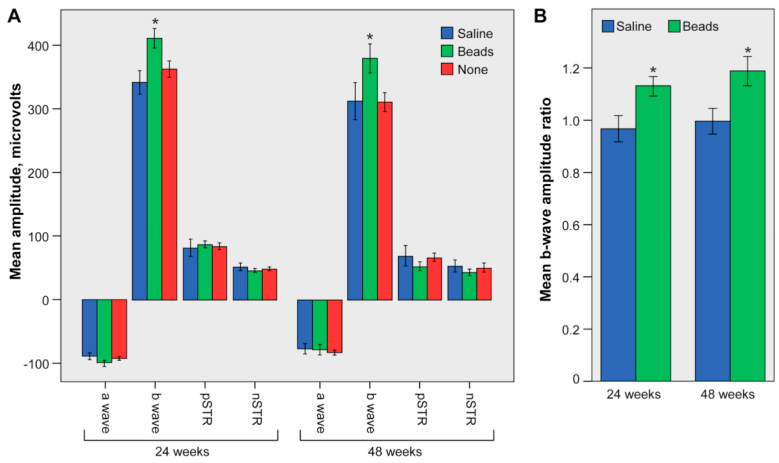

Figure 3. Prolonged IOP elevation results in an increase of the b-wave amplitude

A. Saline-injected (blue), bead-injected (green), and uninjected (red) eyes were included (for 24 weeks, n = 13 for bead-injected eyes, 8 for saline-injected eyes, and 21 for uninjected eyes; for 48 weeks, n = 8 for bead-injected eyes, 5 for saline-injected eyes, and 13 for uninjected eyes). There is a statistically significant increase in the b-wave amplitude of bead-injected eyes at both time points (asterisks). B. The b-wave amplitude ratio is similar in bead-injected (green) eyes compared to saline-injected (blue) eyes at both time points (asterisks). For all panels, an asterisk denotes an ANOVA with repeated measures across light intensities with a p value < 0.05. One SEM is shown.

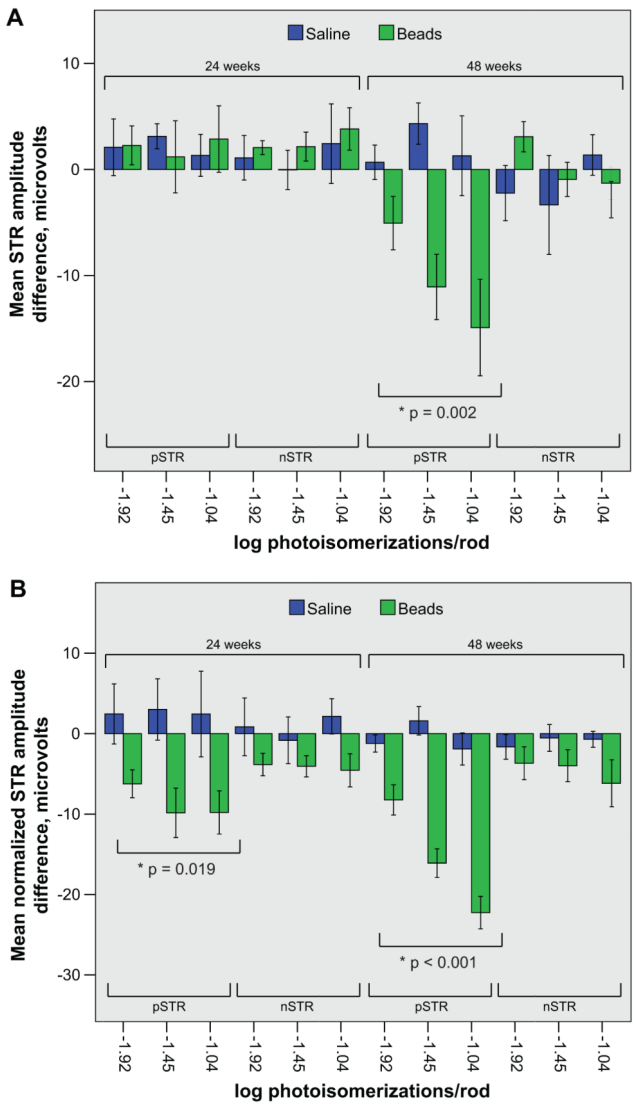

Figure 4. Prolonged IOP elevation results in a decrease of the pSTR amplitude difference

A and B. The mean pSTR and nSTR amplitude difference (lower brackets) following stimulation at three distinct scotopic light intensities (log photoisomerizations/rod) of animals exposed to either 24 or 48 weeks of IOP elevation (upper brackets) is provided. Saline (blue) and bead (green) injected animals of the same exposure duration and light intensity are presented side by side. A. At 24 weeks of IOP exposure there is no reduction in either the pSTR or the nSTR amplitude difference in bead-injected animals when compared to saline-injected animals. However, at 48 weeks of IOP exposure, the pSTR amplitude difference is diminished whereas the nSTR amplitude difference is not. B. At all light intensities at both time points the normalized pSTR amplitude difference is reduced in bead-injected animals when compared to saline-injected animals. For both panels, an asterisk denotes an ANOVA with repeated measures with the indicated p value. One SEM is shown. Note the difference in the scale of the y axis between the two panels.

Table 1

Patterns of IOP Change

IOP data presented according to condition and period of time. Analysis of mean IOP (vs. none) was by ANOVA with repeated measures. Analysis of mean IOP difference was by ANOVA with repeated measures with Bonferroni correction to compare among the 12 week time periods. p-values are as indicated.

Injected, time	IOP (mmHg) I mean ± SD	OP difference (mmHg)		p-value				
		mean ± SD	cumulative mean ± SD	vs. none	vs. weeks 25–48	vs. weeks 13–24	vs. weeks 25–36	vs. weeks 37–48
Beads, weeks 1–48	13.4 ± 4.3	2.7 ± 3.9	138.6 ± 46.9	<0.001				
Beads, weeks 1–24	13.1 ± 4.1	2.2 ± 3.8	56.5 ± 35.4	<0.001	<0.01			
Beads, weeks 25–48	14.0 ± 4.5	3.4 ± 4.3		<0.001				
Beads, weeks 1–12	13.9 ± 4.1	2.6 ± 3.7		<0.001		0.24	1	0.11
Beads, weeks 13–24	12.2 ± 4.1	1.8 ± 3.7		<0.01			0.22	<0.01
Beads, weeks 25–36	13.1 ± 4.2	2.8 ± 4.1		<0.001				0.37
Beads, weeks 37–48	14.8 ± 4.6	4.1 ± 4.3		<0.001				
Saline, weeks 1–48	11.2 ± 3.3	0.8 ± 3.0	37.7 ± 30.9	1				
Saline, weeks 1–24	11.1 ± 3.2	0.7 ± 2.9	16.2 ± 17.8	1				
None, all	10.6 ± 2.8							

Table 2

Mean retinal ganglion cell counts and axial length measurements

RGC counts and axial length measurements were performed at both 24 and 48 weeks after injection. A t-test comparing bead injected eyes to contralateral, uninjected control eyes at the same time point was performed in all cases. p-values are provided in the corresponding text.

Injected, time	RGCs/mm ^{2} mean ± SD	Axial Length (mm) mean ± SD
Beads, 24 weeks	2,454 ± 423 (n = 9)	3.41 ± 0.11 (n = 7)
Beads, 48 weeks	2,985 ± 341 (n = 5)	3.55 ± 0.11 (n = 6)
Control, 24 weeks	2,867 ± 445 (n = 10)	3.27 ± 0.082 (n = 7)
Control, 48 weeks	3,701 ± 439 (n = 5)	3.36 ± 0.12 (n = 6)